AMERICAN SOCIETY FOR MICROBIOLOGY | Applied and Environmental Microbiology®

ENVIRONMENTAL MICROBIOLOGY

Pseudomonas orientalis F9 Pyoverdine, Safracin, and Phenazine Mutants Remain Effective Antagonists against *Erwinia amylovora* in Apple Flowers

Amanda Santos Kron,[a] Veronika Zengerer,[a] Marco Bieri,[a] Vera Dreyfuss,[a] Tanja Sostizzo,[b] Michael Schmid,[c] Matthias Lutz,[d] Mitja N. P. Remus-Emsermann,[e,f] Cosima Pelludat[a]

[a]Agroscope, Research Division Plant Protection, Wädenswil, Switzerland
[b]Agroscope, Research Division Phytosanitary Service, Wädenswil, Switzerland
[c]Genexa AG, Zürich, Switzerland
[d]Agroscope, Research Division Extension Vegetable Growth, Wädenswil, Switzerland
[e]School of Biological Sciences, University of Canterbury, Christchurch, New Zealand
[f]Biomolecular Interaction Centre, University of Canterbury, Christchurch, New Zealand

Amanda Santos Kron and Veronika Zengerer contributed equally to this work. First authorship was determined by alphabetical order.

ABSTRACT The recently characterized strain *Pseudomonas orientalis* F9, an isolate from apple flowers in a Swiss orchard, exhibits antagonistic traits against phytopathogens. At high colonization densities, it exhibits phytotoxicity against apple flowers. *P. orientalis* F9 harbors biosynthesis genes for the siderophore pyoverdine as well as for the antibiotics safracin and phenazine. To elucidate the role of the three compounds in biocontrol, we screened a large random knockout library of *P. orientalis* F9 strains for lack of pyoverdine production or *in vitro* antagonism. Transposon mutants that lacked the ability for fluorescence carried transposons in pyoverdine production genes. Mutants unable to antagonize *Erwinia amylovora* in an *in vitro* double-layer assay carried transposon insertions in the safracin gene cluster. As no phenazine transposon mutant could be identified using the chosen selection criteria, we constructed a site-directed deletion mutant. Pyoverdine-, safracin-, and phenazine mutants were tested for their abilities to counteract the fire blight pathogen *Erwinia amylovora ex vivo* on apple flowers or the soilborne pathogen *Pythium ultimum in vivo* in a soil microcosm. In contrast to some *in vitro* assays, *ex vivo* and *in vivo* assays did not reveal significant differences between parental and mutant strains in their antagonistic activities. This suggests that, *ex vivo* and *in vivo*, other factors, such as competition for resources or space, are more important than the tested antibiotics or pyoverdine for successful antagonism of *P. orientalis* F9 against phytopathogens in the performed assays.

IMPORTANCE *Pseudomonas orientalis* F9 is an antagonist of the economically important phytopathogen *Erwinia amylovora*, the causal agent of fire blight in *pomme* fruit. On King's B medium, *P. orientalis* F9 produces a pyoverdine siderophore and the antibiotic safracin. *P. orientalis* F9 transposon mutants lacking these factors fail to antagonize *E. amylovora*, depending on the *in vitro* assay. On isolated flowers and in soil microcosms, however, pyoverdine, safracin, and phenazine mutants control phytopathogens as clearly as their parental strains.

KEYWORDS *Erwinia amylovora*, *Malus domestica*, biocontrol, cress assay, detached flower assay, fire blight, safracin, siderophore, transposon mutagenesis

The ongoing concerns over the application of pesticides in plant protection intensify the need for management strategies that include the use of antagonists. For their optimal selection and use in agriculture, an understanding of their mode of action is

Citation Santos Kron A, Zengerer V, Bieri M, Dreyfuss V, Sostizzo T, Schmid M, Lutz M, Remus-Emsermann MNP, Pelludat C. 2020. *Pseudomonas orientalis* F9 pyoverdine, safracin, and phenazine mutants remain effective antagonists against *Erwinia amylovora* in apple flowers. Appl Environ Microbiol 86:e02620-19. https://doi.org/10.1128/AEM.02620-19.

Editor Irina S. Druzhinina, Nanjing Agricultural University

Address correspondence to Cosima Pelludat, cosima.pelludat@agroscope.admin.ch.

Received 12 November 2019
Accepted 4 February 2020
Accepted manuscript posted online 7 February 2020
Published 1 April 2020

mandatory. Recently, the antagonistic activity of *Pseudomonas orientalis* F9, an isolate obtained from apple flowers in a Swiss orchard, was tested against several phytopathogenic strains *in vitro* and *ex vivo* (1). *P. orientalis* F9 induced *in vitro* a growth deficiency in the fire blight pathogen *Erwinia amylovora* CFBP1430^{Rif} (*E. amylovora*^{Rif}). The fire blight pathogen affects apple, pear, and quince and is a major threat to fruit production (2). In 2016, the most effective control in fire blight management, the antibiotic streptomycin, was banned from field applications in Switzerland due to the possible rise and spread of resistant pathogens (3, 4). Antagonists are a desirable alternative to antibiotics if their efficacy in reduction of blossom infection is comparable to that of the most effective controls; regardless of the environmental conditions. However, the reduction in blossom infection with biological treatments in experiments conducted between 2001 and 2007 ranged from 9.1 to 36.1% while values for the control with streptomycin ranged from 59 to 67.3% (5). In addition to *E. amylovora*, *P. orientalis* F9 also reduced growth of plant pathogens belonging to pathovars of *Pseudomonas syringae* (*P. syringae* pv. syringae ACW, *P. syringae* pv. actinidiae ICMP 9617, and *P. syringae* pv. persicae NCPPB 2254) in an *in vitro* double-layer assay. However, *ex vivo* on apple flowers, *P. orientalis* F9 revealed phytotoxic properties when inoculated at a high dose (1).

The genome of *P. orientalis* F9 contains genes for the synthesis of pyoverdine (siderophore) and for the synthesis of the antibiotics safracin and phenazine-1-carboxylic acid. Phenazines have an antibiotic activity against bacteria, fungi, and eukaryotes. They are known to successfully suppress soilborne pathogens (6–8). Indeed, when tested in a cress assay, F9 revealed antagonistic activity against the soilborne pathogen *Pythium ultimum* (1). Safracin belongs to the tetrahydroisoquinoline (THIQ) alkaloids, known for their broad-spectrum antibacterial activities (9) and especially strong antitumor activities. The biosynthetic gene clusters of six THIQ antibiotics have been characterized, including ET-743 that has been commercialized as anticancer drug (10). Siderophores are iron chelators that bacteria produce to scavenge iron in iron-deficient environments. Pyoverdines are the fluorescent pigments produced by *Pseudomonas* species and their primary siderophore (11, 12). Siderophores and antibiotics have both been shown to be involved in antagonistic activities against plant pathogens (11, 13). In the present study, we analyzed the antagonistic traits of *P. orientalis* F9 with regard to the siderophore pyoverdine and the antibiotics safracin and phenazine for further understanding and selection of appropriate antagonists.

Transposon mutagenesis and subsequent selection criteria (fluorescence on iron-limited King's B [KB] medium and halo induction of *E. amylovora* in a double-layer assay) led to the identification of pyoverdine and safracin mutants. No phenazine transposon mutant was selected. To exclude the possibility of phenazine as a major player in the antagonistic traits of *P. orientalis* F9, a site-directed mutant of the phenazine cluster of F9 was constructed.

P. orientalis F9 transposon and site-directed mutants were analyzed for their antagonistic activity in order to correlate phenotypic traits of the mutants and their abilities to counteract phytopathogens.

RESULTS

Selected transposon mutants and site of transposon integration. The genome of *P. orientalis* F9 (GenBank accession number CP018049.1) is 5.99 Mbp, with an average GC content of 60.4% and no plasmids. Genome analysis revealed that the genome carries a safracin production cluster, a phenazine-1-carboxylate operon (*phzABCDEFG*) (Fig. 1), and pyoverdine synthesis genes (1).

P. orientalis F9 was subjected to random insertion transposon mutagenesis in order to mutagenize potential antibiotics and siderophore genes. F9 transposon mutants were screened using a double-layer technique on KB agar seeded with *E. amylovora*^{Rif}. Mutants were selected based on their inability to cause growth inhibition halos of the pathogen or on the absence of fluorescence when they were grown on KB plates. The transposon mutants were grouped into two phenotypic groups: no fluorescence/halo induction (nF/H) and fluorescence/no halo induction (F/nH) (Fig. 2).

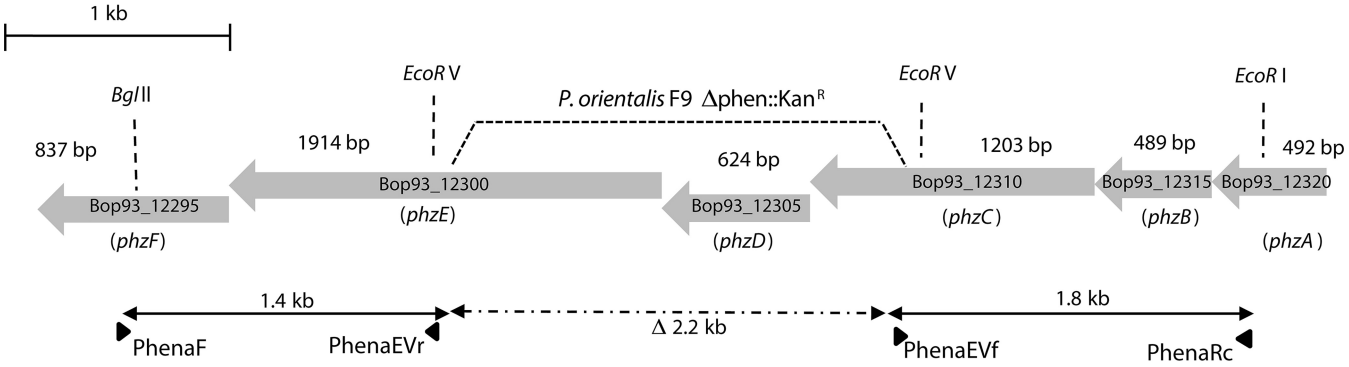

FIG 1 Schematic representation of the phenazine gene cluster in *P. orientalis* F9. Large gray arrows indicate coding sequences. Small black horizontal arrows show positions and directions of primers used for site-directed mutagenesis. The PCR-generated fragments were cut at naturally occurring EcoRV restriction sites for insertion of the kanamycin resistance cassette, leading to deletion of a 2.2-kb fragment of the phenazine cluster in *P. orientalis* F9 (Δphen::Kan^r). Genes were assigned with their corresponding accession numbers from the sequenced *P. orientalis* F9 genome and correspond to the six genes *phzABCDEF* of the phenazine cluster (from right to left).

The insertion site of the transposon on the *P. orientalis* F9 chromosome was determined for 15 mutants of group 1 (nF/H) and 4 mutants of group 2 (F/nH) using arbitrary PCR. All nF/H mutants carried the transposons within the 19 genes predicted to be part of the pyoverdine synthesis cluster, and F/nH mutants carried the transposons within the 10 genes with high similarity to the safracin cluster in *Pseudomonas fluorescens* A2-2 (9).

Nine of the nF/H selected transposon mutants carried their transposons in Bop93_18020, which encodes a protein with 91% amino acid identity to PvdL, a pyoverdine chromophore precursor synthetase of the fluorescent bacterium *Pseudomonas synxantha* BG33R. Transposon mutants TM8, TM14, TM15, TM16, and TM17 shared the same insertion site in Bop93_18020, possibly due to clonal origin, while TM13 and TM38 carried their transposons closer to the 3′ end of the gene (Fig. 3A). Mutant TM10 (nF/H; data not shown) carries the transposon in BOP93_10425, a gene with homology to *pvdF* encoding the pyoverdine synthetase of *Pseudomonas protegens* Pf-5 (PFL_4090).

TM18 (F/nH) carries an insertion in Bop93_17405. Bop93_17405 encodes a protein that is more than 78% amino acid identical to SfcA, which is part of the safracin cluster in *P. fluorescens* ATCC 13525. TM19 (F/nH) is a transposon mutant of Bop93_17410 which is also part of the safracin cluster (*sfcB*) (Fig. 3B; Table 1). An additional F/nH mutant was detected with the transposon insertion in Bop93_17440 which encodes a protein that has identity to SfcH (85%). For subsequent analyses in various assays, TM16 and TM18 as representative of each phenotypic group were selected.

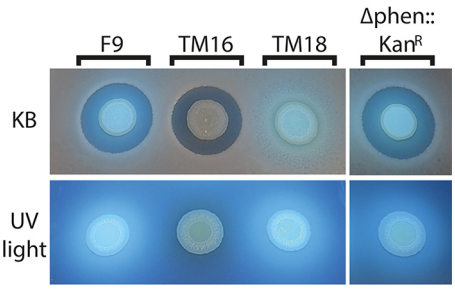

FIG 2 Double-layer assay with *P. orientalis* F9 (F/H), transposon mutants TM16 (nF/H) and TM18 (F/nH), and phenazine mutant *P. orientalis* F9 (Δphen::Kan^r) (F/H) pipetted onto *E. amylovora* CFBP1430 seeded in KB overlay agar. Presence and absence of *E. amylovora* inhibition zones are visualized in the KB medium double-layer assay; UV light reveals the presence or absence of the fluorescence that is indicative for siderophore production. nF/H, no fluorescence/halo induction; F/nH, fluorescence/no halo induction; F/H, fluorescence/halo induction.

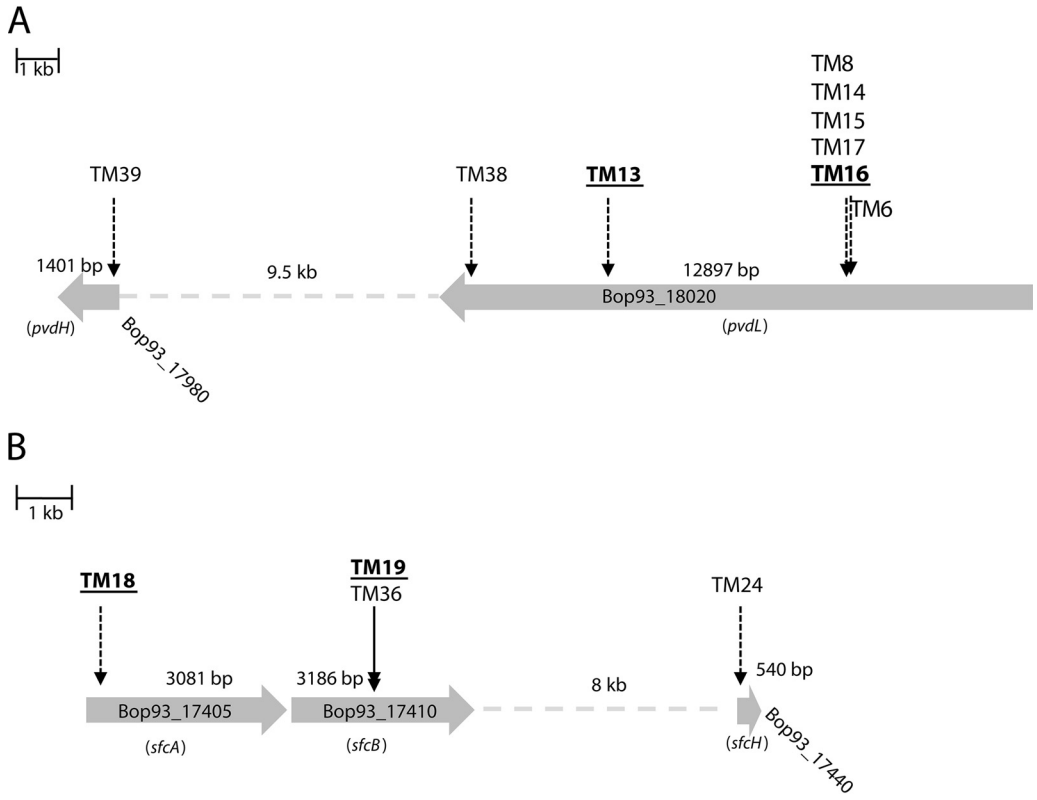

FIG 3 Schematic representation of transposon location for each defined phenotype group. Coding sequences are indicated by large horizontal arrows which show the directions of transcription. Black vertical arrows show the integration sites of transposons. Dashed lines represent intermediate DNA regions (length in kilobases). Genes were assigned to the annotated *P. orientalis* F9 genome with their corresponding Bop number. (A) Transposon location of fluorescence-negative but halo-inducing mutants (nF/H) in genes Bop93_17980 and Bop93_18020. Homology study allocated the two genes to the pyoverdine gene cluster. TM16 and TM13 were used in further analysis. (B) Transposon location of fluorescent but not halo-inducing mutants (F/nH). Insertion occurred in three different genes of the safracin cluster. TM18 and TM19 were used in further analysis.

No transposon mutant with an insertion in the phenazine gene cluster was identified. Thus, site-directed mutagenesis was performed, leading to a 2.2-kb deletion in the phenazine operon in *P. orientalis* F9 (here, the Δphen::Kan^r strain). The mutant strain showed fluorescence when grown on KB plates and *E. amylovora* halo induction in the double-layer assay (F/H phenotype) (Fig. 1 and 2; Table 1).

Growth of *P. orientalis* F9 and corresponding mutants in PSBM and KB medium. The growth of *P. orientalis* F9 and its mutants was evaluated in partial stigma-based medium (PSBM) (14), which mimics the nutrient composition on the stigma, and in iron-limited KB medium. In PSBM, TM16 showed less growth than TM18, F9 (Δphen::Kan^r), or the parental strain. In KB medium all strains grew equally well (Fig. 4). When tested on siderophore indication agar (chrome azurol S [CAS] agar), all strains, including TM16, produced halos of the same size (see Fig. S1 in the supplemental material). The CAS phenotype and growth of TM16 in KB medium indicate an additional siderophore system present in *P. orientalis* F9. However, genome analysis of F9 failed to identify additional secondary siderophores (yersiniabactin, pyochelin, achromobactin, PDTC [pyridine-2,6-bis(monothiocarboxylic acid)], or thioquinolobactin).

Ability of F9 transposon mutants to inhibit growth of phytopathogens and antagonists *in vitro*. A previous study demonstrated that *P. orientalis* F9 is capable of inhibiting the growth of bacterial phytopathogens and antagonists *in vitro* (1). Strains *E. amylovora*^{Rif}, the *E. amylovora* antagonist *Pantoea vagans* C9-1, *P. syringae* pv. syringae ACW, *P. syringae* pv. actinidiae ICMP 9617, and *P. syringae* pv. persicae NCPPB 2254 (15–17) were poured into the top layer of a double-layer assay. The assay revealed

TABLE 1 Strains and plasmids used in this study

Strain or plasmid	Notes[a]	Reference or source
Strains		
P. orientalis F9 strains		
Wild type	Isolated from *Malus domestica* flower, canton Zurich, Switzerland, in 2014; F/H	1
TM10	Transposon mutant of F9; nF/H	This study
TM13	Transposon mutant of F9; nF/H	This study
TM16	Transposon mutant of F9; nF/H	This study
TM18	Transposon mutant of F9; F/nH	This study
TM19	Transposon mutant of F9; F/nH	This study
Δphen::Kan^r strain	Phenazine mutant F9 with deletion of *phzCDE*; F/H	This study
E. amylovora CFBP1430^{Rif}	Spontaneous rifampicin-mutant of *E. amylovora* CFBP1430	1
P. vagans C9-1	*E. amylovora* antagonist	16
P. syringae pv. persicae NCPPB 2254	Causal agent of bacterial die-back in peach, nectarine, Japanese plum	CFBP[b]
P. syringae pv. actinidiae ICMP 9617	Causal agent of bacterial canker of kiwifruit	CFBP
P. syringae pv. syringae ACW	Causal agent of bacterial canker of *pomme* and stone fruit	1
P. protegens CHA0	Model organism in biological control of soilborne pathogens	51
E. coli S17-1 λpir	*pir*$^+$ *tra*$^+$, Sm^r	52
E. coli SM10 λpir(pJA1)	Contains the suicide vector pJA1; *pir*$^+$ *tra*$^+$, Kan^r	52
P. ultimum	Soilborne phytopathogen	51
Plasmids		
pKAS32	Cloning vector with *rpsL* gene, Amp^r	42
pSB315	Containing kanamycin cassette without transcriptional terminator, Amp^r Kan^r	43
pJA1	Containing transposon, Kan^r	37

[a]F/H, fluorescence/halo induction; nF/H, no fluorescence/halo induction; F/nH, fluorescence/no halo induction.
[b]CFBP, Collection Française de Bactéries associées aux Plantes.

that the nonfluorescent TM16 mutant (nF/H) and *P. orientalis* F9 (Δphen::Kan^r) (F/H) induced a growth deficiency similar to that of the parental strain *P. orientalis* F9. The fluorescent but safracin-negative mutant TM18 (F/nH), on the other hand, had no impact on the growth of the tested strains (Fig. 5).

Ability of F9 transposon mutants to inhibit growth of *P. ultimum* in a cress assay. A cress assay was performed with *P. orientalis* F9 and mutant strains. As shown previously (1), *P. orientalis* F9 was similarly effective as the established antagonist *P. protegens* CHA0 (Fig. 6B) when cress was coinoculated with the soilborne pathogen *P. ultimum* in soil. *P. orientalis* F9 and its mutants were applied onto soil containing *P. ultimum* and cress. Transposon mutants TM16, TM18, and *P. orientalis* F9 (Δphen::Kan^r) exhibited no statistically significant difference compared to results with the parental strain (Fig. 6A and B).

Growth inhibition of *E. amylovora*^{Rif} in an *in vitro* competition assay using stigma-based medium. *P. orientalis* F9 originates from apple flowers, and despite its phytopathogenic traits in the flower, the strain also significantly reduces *E. amylovora*^{Rif} CFU counts on flowers. To elucidate whether or not siderophore and safracin deficiency has an impact on antagonistic activity *in vitro*, a PSBM competition assay was per-

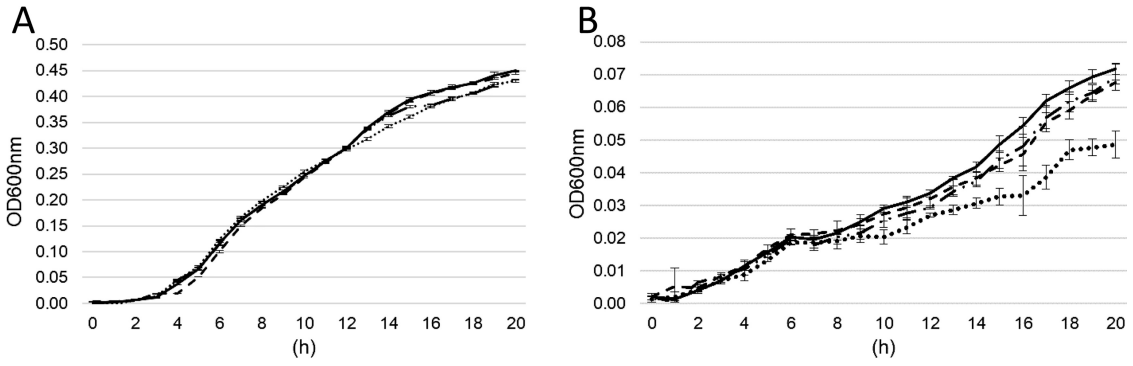

FIG 4 Growth curve of *P. orientalis* F9 (black line), *P. orientalis* F9 (Δphen::Kan^r) (broken line), nF/H mutant TM16 (dotted line), and F/nH mutant TM18 (dotted broken line) in KB medium (A) and PSBM (B). Error bars represent standard deviations.

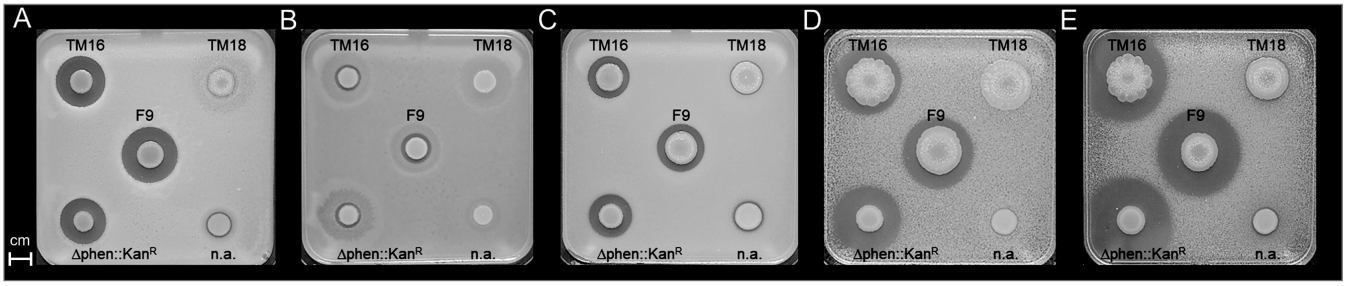

FIG 5 Double-layer assay of *P. orientalis* F9 and corresponding mutant strains and their impact on the growth of plant pathogens and antagonists seeded in a KB medium overlay. (A) *E. amylovora* CFBP1430. (B) *P. vagans* C9-1 (*E. amylovora* antagonist). (C) *P. syringae* pv. syringae ACW. (D) *P. syringae* pv. actinidiae ICMP 9617. (E) *P. syringae* pv. persicae NCPPB 2254. The following strains were spotted on top: *P. orientalis* F9, *P. orientalis* F9 (Δphen::Kan^r), nF/H mutant TM16, and F/nH mutant TM18, as indicated. n.a., not applicable.

formed. PSBM mimics nutrients present on the stigma. *E. amylovora*^{Rif} was coinoculated with *P. orientalis* F9 or transposon mutants. *E. amylovora*^{Rif} CFU counts were determined after 3 and 4 days of incubation. In contrast to results from the double-layer assay with KB medium, the nonfluorescent mutant TM16 revealed reduced antagonistic activity against the fire blight pathogen, which is in accordance with PSBM growth curve results (Fig. 4B), in which TM16 showed reduced growth. There was no significant difference in the CFU counts of *E. amylovora*^{Rif} coinoculated with *P. orientalis* F9 or the safracin mutant TM18 (Fig. 7).

Inhibition of *E. amylovora*^{Rif} by *P. orientalis* F9 mutants in a detached-flower assay. Flowers are the primary location in which *E. amylovora* replicates and subsequently invades the plant host tissue. Thus, growth reduction of *E. amylovora* in the flowers is one of the most important tasks of fire blight management. To evaluate the impact of pyoverdine, phenazine, and safracin on the antagonistic activity of *P. orientalis* F9 against *E. amylovora*^{Rif} in the apple flower, a detached-flower assay was performed. *P. orientalis* F9 and transposon mutants TM16 (nF/H) and TM18 (F/nH) as well as the deletion mutant *P. orientalis* F9 (Δphen::Kan^r) were coinoculated with *E. amylovora*^{Rif} onto the hypanthium of apple flowers. After 2 and 4 days of incubation, *E. amylovora*^{Rif} was reisolated from the apple flowers, and the CFU counts were determined on selective medium. No significant difference in the determined CFU counts could be detected (Fig. 8A and B). This was also true for alternative transposon mutants TM13 (nF/H), TM19 (F/nH), and TM10 (nF/H) (Fig. 8C and D).

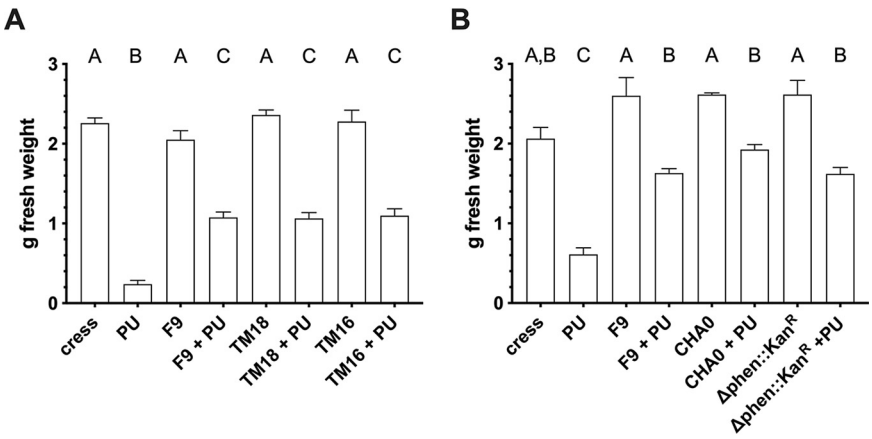

FIG 6 (A) Cress biomass after treatment with *P. ultimum* (PU) and/or *P. orientalis* F9 and corresponding transposon mutants TM18 and TM16. (B) Cress biomass after treatment with *P. ultimum* (PU) and/or *P. orientalis* F9, *P. orientalis* F9 (Δphen::Kan^r), and known antagonist *P. protegens* CHA0, as indicated. Cress biomass was harvested at 7 days postinoculation. Error bars depict the standard errors of the means. Different letters depict significant differences between measurements (one-way analysis of variance and multiple-comparison test with Tukey's correction, $P < 0.0001$).

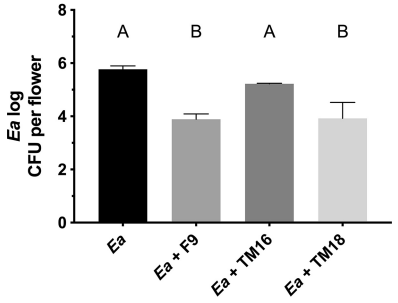

FIG 7 *In vitro* competition assay of *P. orientalis* F9 and transposon mutants TM16 (nF/H) and TM18 (F/nH), cocultivated with *E. amylovora*^{Rif} (*Ea*) in PSBM at 26°C. *E. amylovora*^{Rif} CFU counts were determined after 3 days of incubation. Error bars represent standard deviations of the means. Different letters depict significant differences between measurements (one-way analysis of variance and multiple-comparison test with Tukey's correction, $P < 0.05$).

Thus, in the detached-apple flower assay, the parental *P. orientalis* F9 strain and all tested mutants had the same antagonistic activities against the fire blight pathogen. In addition, when *P. orientalis* F9, TM16, and TM18 and *P. orientalis* F9 (Δphen::Kan^r) were inoculated solely with a high inoculum in apple flowers, all strains revealed phytotoxic effects (Fig. S2). Thus, in the performed detached-flower assay, neither the siderophore nor the tested antibiotics are major participants in antagonistic traits or necrosis of apple flowers.

DISCUSSION

P. orientalis F9 has been shown to reduce growth of phytopathogenic microorganisms *in vitro* and *ex vivo* (1). We analyzed the impact of the strain's antibiotics safracin and phenazine as well as its siderophore pyoverdine on its antagonistic traits.

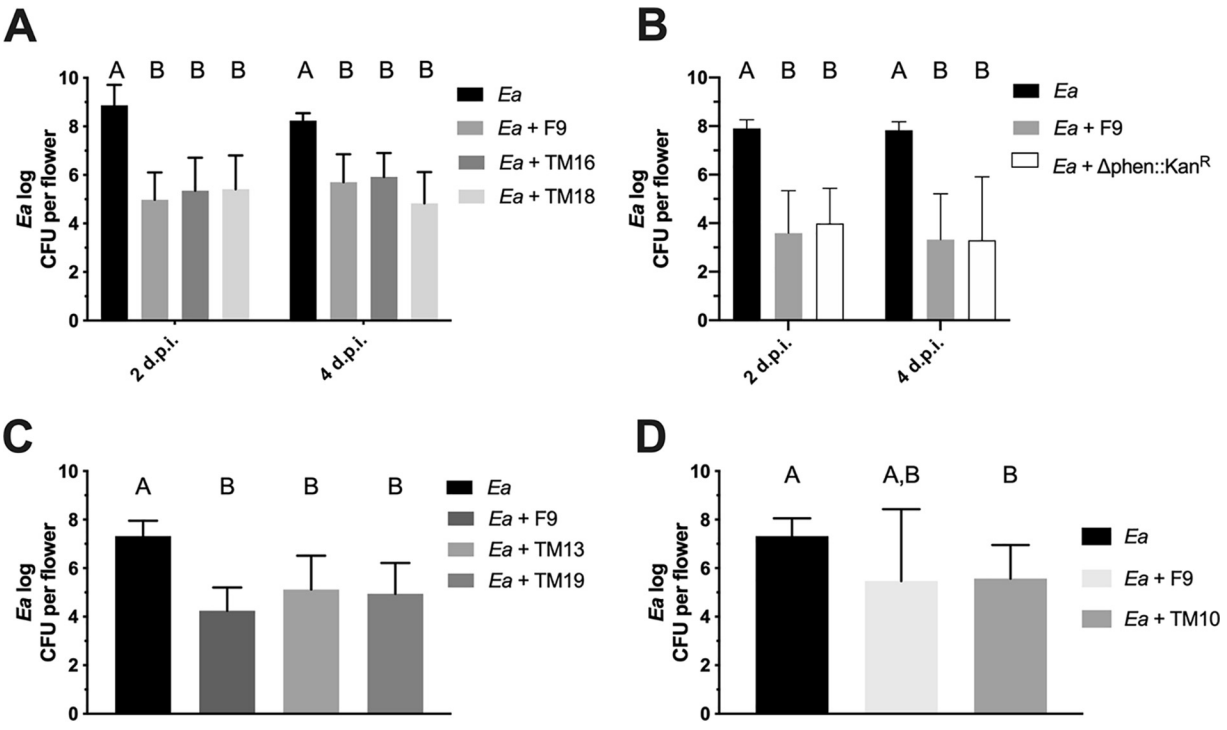

FIG 8 Antagonistic activity of *P. orientalis* F9 and mutants against *E. amylovora*^{Rif} (*Ea*) in apple flowers. (A and B) Recovered CFU counts (log) of *E. amylovora*^{Rif} control and *E. amylovora*^{Rif} coinoculation with *P. orientalis* F9, nF/H mutant TM16), and F/nH mutant TM18 or *P. orientalis* F9 (Δphen::Kan^r) after 2 and 4 days postinfection. (C and D) Antagonistic activity of *P. orientalis* F9 alternative mutants TM13 (nF/H) and TM19 (F/nH) and TM10 (nF/H), as indicated, at 5 days postinfection. Error bars represent standard deviations of the means. Different letters depict significant differences between measurements (two-way analysis of variance and multiple-comparison test with Tukey's correction, $P < 0.005$).

The main siderophores produced under iron-limiting conditions by fluorescent pseudomonads, including *P. orientalis* F9, are pyoverdines. Thus, transposon mutants of *P. orientalis* F9 were selected according to their loss of fluorescence on iron-limited KB plates, indicative of the absence of pyoverdine. Additionally, mutants that exhibited loss of growth halo induction were selected using a double-layer assay with *E. amylovora*^{Rif} seeded as an indicator strain in a top layer of KB medium. Halo-inducing negative mutants were shown to carry transposon insertions within genes of the safracin operon (Fig. 3B, TM18 and TM19). TM16, TM13, and TM10 represented the nonfluorescent, but halo-forming phenotype, with the transposon inserted in the pyoverdine synthesis genes (Fig. 3A). As no transposon insertion in the annotated phenazine synthesis genes of *P. orientalis* F9 could be identified, site-directed mutagenesis was performed, resulting in *P. orientalis* F9 (Δphen::Kan^{r}) (Fig. 1).

In the double-layer assay using KB medium, nonfluorescent mutant TM16 revealed growth reduction not only of *E. amylovora*^{Rif} but also of *P. syringae* pathovars and the *E. amylovora* antagonist *P. vagans* C9-1, similar to results with the wild type. The same was true for *P. orientalis* F9 (Δphen::Kan^{r}) (Fig. 5). In contrast, the fluorescent mutant TM18 with the transposon positioned in the *sfcA* homolog of F9 was incapable of inducing a halo in any of the seeded strains (Fig. 5). This indicates that in this assay the production of safracin is sufficient to negatively impact growth of the tested strains. Therefore, the antagonistic activity of *P. orientalis* F9 in the double-layer assay can be attributed to the production of safracin but not to that of pyoverdine or phenazine. In contrast, when strains were tested in an *in vitro* competition assay in PSBM, which mimics the nutrient composition of the stigma (14), only the siderophore-negative mutants TM16 (Fig. 7) and TM13 (data not shown) failed to reduce the CFU count of *E. amylovora*^{Rif}. This is in correspondence with the weaker growth of TM16 in PSBM than that of the other strains (Fig. 4).

When tested in the *in vivo* cress assay and in the *ex vivo* detached apple flower assay, the *P. orientalis* F9 mutants have the same antagonistic activity against *E. amylovora*^{Rif} and the model soil pathogen *P. ultimum* as the parental strain (Fig. 6 and 8). The recovered CFU counts of *E. amylovora*^{Rif} after coinoculation into apple flowers with *P. orientalis* F9, corresponding transposon mutants TM16 and TM18, alternative transposon mutants TM13, TM10, and TM19, or *P. orientalis* F9 (Δphen::Kan^{r}) did not differ significantly (Fig. 8). The same was true for the cress biomass defined after coinoculation of the pathogen with parental or mutant strains (Fig. 6). *E. amylovora* produces the hydroxamate siderophore desferrioxamine E (DFO E) (18–20). The importance of this system for the pathogenicity of *E. amylovora* has been demonstrated using mutants deficient in siderophore synthesis or uptake (21). The lack of pyoverdine production in TM16 and the subsequent reduced competition of the mutant strain for iron in the apple flower were expected to impact its ability to counteract *E. amylovora*. Thus, it was unexpected that TM16 was still able to significantly reduce *E. amylovora*^{Rif} in the detached-flower assay. When poured on CAS agar, TM16 produced a halo (indicative for siderophore synthesis) (see Fig. S1 in the supplemental material) equal in size to that of parental strain F9. Genome analysis could not reveal additional synthesis genes for secondary siderophores such as yersiniabactin, pyochelin, achromobactin, PDTC, or thioquinolobactin. Either F9 carries an unidentified system, or the CAS assay interferes with alternative iron chelating agents, e.g., citrate that triggered the CAS signal in case of *Bradyrhizobium japonicum* and enabled the strain to take up iron (22). In case of the marine pathogen *Photobacterium damselae* subsp. *damselae*, a mutant lacking the citrate synthase (GltA) showed almost no reaction in the CAS test (23). The *P. orientalis* F9 chromosome encodes a protein with 72.5% identity. In addition, phenazine-1-carboxylic acid production also has an impact on iron availability; e.g., strains producing the antibiotic can have an enhancing effect on the reactivity and mobility of iron derived from soil minerals (24). The reason why the results of the double-layer assay and of the competition in liquid PSBM contradict each other is unknown. Potentially, the experimental conditions in the two assays select for different transcriptional activities in *P. orientalis* F9. Siderophore production is regulated by Fe^{2+} concentration

in the cell (25, 26), while the regulation of safracin production is unknown. Generally, antibiotic production has been shown to be regulated not only via quorum sensing (QS) but also by the presence and absence of interspecies competition (27, 28). Genes coding for proteins with high similarity to the LasI/R and RhlI/R QS systems that regulate the production of multiple virulence factors in *P. aeruginosa* (29) could not be detected in *P. orientalis* F9.

Safracin has been shown to be a broad-spectrum antibiotic (30) and, indeed, caused strong inhibition *in vitro*. However, it appears to have a minor role or no role in competition against *E. amylovora*^{Rif} in detached flowers or against *P. ultimum* in soil. There are additional metabolites that are major candidates for the antagonistic performance of *P. orientalis* F9 in the *in vivo* assays. The strain also harbors poaeamide (BOP93_16455) and obafluorin synthesis genes on its genome. Poaeamide inhibited mycelial growth of *Rhizoctonia solani* and different oomycetes, including *P. ultimum* (31). This might explain why the phenazine deletion mutant of F9 is still able to antagonize *P. ultimum* in the cress assay. The β-lactone antibiotic obafluorin produced by *P. fluorescens* ATCC 39502 showed weak antibacterial activity against a range of bacteria by disk diffusion (32). In addition, *P. orientalis* F9 also harbors genes with homology to the Hcp secretion island 1-encoded type VI secretion system (H-T6SS) (BOP93_RS26545 to BOP93_RS26640). In the case of *Serratia marcescens* Db10, the T6SS exhibits antibacterial killing activity (33). Future analyses have to determine if these features of *P. orientalis* F9 are major players in the strain's repertoire of antagonistic traits in the apple blossom or cress assay.

Results presented in this paper demonstrate that competition and antagonism are multifactorial and not solely dependent on antibiotic and/or siderophore production. Investigating the causal reason for the different results is, however, out of the scope of this study. The actual cause for antagonism is thus still unclear and could be mediated by the plant host, resource competition, or antibiotics that have not been studied (28, 34, 35). Our results highlight the importance of a proper choice of screening systems that need to be sufficiently close to environmental conditions. Results of *in vitro* screens do not reflect *in situ* results and need to be supplemented by additional corroborative assays.

MATERIALS AND METHODS

Cultivation of bacterial strains used. Bacterial overnight cultures were grown at 26°C in tryptic soy broth (TSB; Oxoid, Karlsruhe, Germany) or King's B (KB) medium (36). Partial stigma-based medium (PSBM) (14) was also used. Microorganisms used in the study are listed in Table 1. Where appropriate, medium was supplemented with kanamycin or rifampin at a concentration of 40 mg liter^{-1} or 100 mg liter^{-1}, respectively.

Transposon mutagenesis. Random insertion Tn*10* transposon mutagenesis was performed using pJA1, an oriR6K-based suicide vector. The plasmid contains the Tn*10* transposase and confers kanamycin resistance (37). Donor *Escherichia coli* SM10 λpir(pJA1) and recipient *P. orientalis* F9 were grown overnight in either LB medium (10 g liter^{-1} tryptone, 5 g liter^{-1} yeast extract, 10 g liter^{-1} NaCl, pH 7.0 ± 0.2 [Carl Roth]) supplemented with kanamycin or KB medium, respectively. The overnight culture of *E. coli* SM10 λpir(pJA1) was inoculated into fresh LB medium containing kanamycin and grown to mid-exponential phase. One milliliter of the donor and the recipient in stationary phase was mixed and centrifuged for 30 s at 10,000 × *g*. The bacterial pellet was washed twice with 1× phosphate-buffered saline (PBS) (2.5 g liter^{-1} K_2HPO_4, 1.2 g liter^{-1} KH_2PO_4) and subsequently spotted onto the center of an isopropyl-β-D-thiogalactopyranoside (IPTG)-containing LB plate (10 μl of a 100 mM IPTG solution, spotted onto the center of the plate). The conjugation plate was incubated at 37°C for 3 to 5 h. A dilution series was plated onto MM2-agar plates (4 g liter^{-1} L-asparagine, 2 g liter^{-1} K_2HPO_4, 0.2 g liter^{-1} $MgSO_4$, 3 g liter^{-1} NaCl, 10 g liter^{-1} sorbitol, 15 g liter^{-1} agar) supplemented with kanamycin. After 2 to 3 days of growth at 26°C, single colonies were picked and inoculated in 96-well plates containing KB medium and grown for 2 days at 26°C. *P. orientalis* F9 mutants were screened for two phenotypes: (i) a lack of fluorescence in the iron-limited KB agar and (ii) a lack of growth deficiency halos on KB plates overlaid with *E. amylovora*^{Rif} in the double-layer assay (see below).

Identification of transposon insertion sides. Transposon insertion sites were identified according to Holenstein (38). As previously described (39), transposon insertion-specific primers arPCR-T7 (5′-GCA CCTAACCGCTAGCACGTATACGACTC-3′) and ARB6 (5′-GGCCACGCGTCGACTAGTACNNNNNNNNNNACGC C-3′) were used for a primary PCR. In a second, nested PCR, primers arPCR-T7 inner (5′-TGAACGGTAG CATCTTGACGAC-3′) and ARB2 (5′-GGCCACGCGTCGACTAGTAC-3′) were used. A crude DNA extract of selected transposon mutants was prepared by suspending 24- to 48-h-old bacterial colonies in 300 μl of double-distilled H_2O and incubating them at 95°C for 30 min, followed by centrifugation at 12,000 × *g* for 1 min. The supernatant was diluted 1:10 with double-distilled H_2O and used as a PCR template.

Amplifications were performed using Hotstar *Taq* polymerase (Qiagen). PCR products were sequenced using an ABI Prism BigDye Terminator, version 1.1, cycle sequencing kit (Applied Biosystems) and analyzed using nucleotide NCBI (National Center for Biotechnology Information) BLAST against the *P. orientalis* F9 whole-genome sequence (1) and protein BLAST using the UniProt database with default settings (40).

Site-directed mutagenesis of *P. orientalis* F9. A phenazine mutant of *P. orientalis* F9 (Δphen::Kan^r) was generated by site-directed mutagenesis. For this purpose, the BglII, EcoRI, and EcoRV cut sites within the phenazine gene cluster (Fig. 1) were used. Two fragments of ca. 1.4 kb (primer PhenaF, 5′-GTCGTG GAAGCTGGACAGTG-3′; primer PhenaEVr, 5′-GACTCGGCGATCCTGATTCG-3′; annealing temperature of 58°C) and 1.8 kb (primer PhenaEVf, 5′-TGGTGTTGCCGTGCATCGGG-3′; primer PhenaR, 5′-AACCGGTGAA CCCCTTGTTT-3′; annealing temperature of 58°C) of a 5.2-kb BglII/EcoRI fragment of the phenazine gene cluster were amplified by PCR. The 1.4-kb PCR product was digested with BglII/EcoRV, and the 1.8-kb product was digested with EcoRV/EcoRI. The BglII/EcoRV product was ligated in a first step into the similarly digested suicide vector pKAS32 (41), followed by ligation with the EcoRV/EcoRI-digested 1.8-kb fragment and the appropriate cut vector of the first ligation step. The resulting plasmid pSVI1 + 2 harbored the 5′ and 3′ end flanking regions of the BglII/EcoRI phenazine fragment with a 2.2-kb deletion in between. pSVI1 + 2 was EcoRV digested and ligated with a HindII-cut kanamycin cassette from pSB315 (42), resulting in pSVKan. When pKAS32 derivatives are used for the positive selection of a double-allelic exchange, a streptomycin-resistant parental strain is required (41). Spontaneous streptomycin-resistant colonies of *P. orientalis* F9 were isolated by increasing streptomycin concentrations (starting concentration of 10 μg/ml; final concentration of 100 μg/ml) in KB medium. pSVKan was conjugated into *P. orientalis* F9 (Sm^r) using two-parental mating employing *E. coli* S17-1 λpir (43). Kanamycin- and streptomycin-resistant mutants were selected on MM2 medium containing 40 μg/ml kanamycin and 500 μg/ml streptomycin. Strain *P. orientalis* F9 (Δphen::Kan^r Sm^r) was tested via PCR using primers for the presence of the kanamycin resistance gene (aph157, 5′-GTCACCGAGGCAGTTCCA-3′; aph606, 5′-CGACC ATCAAGCATTTTATC-3′; annealing temperature of 58°C) and primers set before the EcoRV restriction site (DelF, 5′-AGGTGAACGTGTCTTCGGCG-3′; DelR, 5′-CTCCCGATCATGTGATCCGC-3′). DelF and DelR amplified a ca. 700-bp fragment and the integrated kanamycin resistance cassette. The position of the kanamycin cassette within the former EcoRV cutting site was confirmed by sequencing.

Bacterial growth rate analysis. For growth rate analysis, a Bioscreen C (Oy Growth Curves Ab, Ltd., Helsinki, Finland) automatic microbiology growth curve analysis system was used. Nine hundred millimeters of medium (KB or PSBM) was pipetted into a reaction mixture, 200 μl of which was not inoculated but used as a negative control for the corresponding growth curves. The remaining 700 μl was inoculated with 3 μl of overnight culture of the tested strain. Three replicates of the inoculated medium, each 200 μl, were loaded in wells of a Bioscreen C honeycomb plate. The plates were incubated at 26°C for 24 h and were shaken every 20 min for 10 s before the absorbance at an optical density of 600 nm (OD_{600}) was determined. Growth experiments were performed in two independent trials.

Siderophore assay. Siderophore production was tested using chrome azurol S (CAS) agar (44). Bacteria were grown overnight on TSB plates, harvested, and resuspended in PBS to an OD_{600} of 1. Five microliters of the bacterial suspension was spotted onto chrome azurol S agar and incubated for 3 days at 26°C. Siderophore-producing strains induce a color change from a green-blue CAS-iron complex to orange desferrated CAS.

Phytotoxicity test of *P. orientalis* F9 and mutant strains. For the phytotoxicity test, *P. orientalis* F9 and mutant strains were cultivated overnight on TSB plates. Colonies were resuspended in 1× PBS and adjusted to an OD_{600} of 1. Twenty microliters of a 10^{-2} dilution of the suspension was applied onto the hypanthium of apple flowers. Inoculated flowers were incubated at 26°C in closed boxes with water-saturated paper towels, and necrosis was evaluated 4 days postinfection (dpi).

Growth inhibition test using a double-layer assay. For a double-layer assay, the strains were cultivated overnight on KB plates. Colonies were resuspended in 1× PBS and adjusted to an OD_{600} of 1. For bacteria seeded in the top layer, approximately 5×10^8 bacteria were added to 10 ml of 0.75% KB top agar (cooled to 45°C). Fifteen milliliters of a top agar was poured on top of a 12 cm by 12 cm KB agar plate. Ten microliters of each *P. orientalis* F9 mutant strain tested as an antagonist was spotted onto the solidified top layer surfaces. Growth halos were detected after 2 days of incubation at 26°C.

Stigma-based medium *in vitro* competition assay. *E. amylovora*^{Rif}, *P. orientalis* F9, and mutants were cultivated on KB plates overnight. Colonies were harvested and resuspended in 1× PBS to an OD_{600} of 1 before being serially diluted up to 10^{-4}. Twenty microliters of this bacterial suspension was then added to 980 μl of 1× PBS, or, in the case of a coinoculation, 20 μl of each strain was added to 960 μl of 1× PBS. Sixty microliters of the bacterial suspension was directly pipetted into 1,440 μl of PSBM, vortexed, and then aliquoted to 400 μl in three columns of a 96-deep-well plate. After 3 days at 26°C, the CFU counts of *E. amylovora*^{Rif} were determined. A serial dilution of the inoculated medium was performed up to 10^{-7}. Three microliters of each dilution was spotted onto TSB plates supplemented with rifampin (100 μg/ml). Experiments were repeated three times independently.

Cress assay. For the cress assay (45), two 1-cm-diameter discs of *Pythium ultimum* culture grown on malt extract agar (Oxoid) were punched out, laid on the bottom of a 9-cm-diameter petri dish, and carefully overlaid with 14 g of doubly autoclaved soil. *P. orientalis* F9 and F9 mutants were grown on KB plates overnight and resuspended in 1× PBS to an OD_{600} of 0.1. Ten milliliters of the bacterial suspensions or mock control (PBS only) was evenly spread over the soil surface, followed by 0.4 g of cress seeds (*Lepidium sativum*). Petri dishes were incubated at 22°C and 65% humidity. After 2, 4, and 6 days of incubation, 20 ml of autoclaved water was added. After 7 days of incubation, the complete above-ground cress biomass was harvested, and its wet weight was determined. Each treatment was performed

in duplicates for inoculation of cress only with *P. orientalis* F9, TM16, TM18, *P. orientalis* F9 (Δphen::Kan^r), and *P. protegens* CHA0 or in quadruplicates for *P. ultimum* controls and coinoculations of *P. orientalis* F9, TM16, TM18, *P. orientalis* F9 (Δphen::Kan^r), and *P. protegens* CHA0 with *P. ultimum*. The experiments were repeated two to three times independently.

Detached-flower assay. For the detached-flower assay (46), freshly opened flowers of 2-year-old potted *Malus domestica* Golden Delicious in the greenhouse were used. *E. amylovora*^{Rif}, *P. orientalis* F9, and mutants were cultivated and resuspended to an OD_{600} of 1 as described above. A serial dilution of each bacterial suspension was performed. For the *E. amylovora* control, 20 μl of the 10^{-4} dilution was transferred into 980 μl of PBS; for coinoculations, 20 μl of each strain was transferred into 960 μl of PBS. Twenty microliters of the bacterial suspensions was directly pipetted onto the hypanthium of individual flowers. Mock treatments were performed with 1× PBS. After inoculation, flowers were incubated at 26°C in closed boxes with water-saturated paper towels on the bottom. Two and four days postinfection (dpi), the CFU counts of *E. amylovora*^{Rif} in eight individual flowers of each treatment were determined as described previously (1). Briefly, petals, pedestals, stamens, and stigmas of the flowers were removed, and the remaining flowers were shaken in 1 ml of 1× PBS for 30 min at 1,400 rpm. Afterwards, tubes were vortexed for 30 s. A serial dilution of the supernatant suspension was performed up to 10^{-7}, and 3 μl of each dilution was spotted onto TSB plates supplemented with rifampin (100 μg/ml). Detached-flower assays for transposon mutants TM16 and TM18 (and alternative mutants TM10, TM13, and TM19) were performed during the spring and summer of 2018, and for the phenazine mutant *P. orientalis* F9 (Δphen::Kan^r), they were performed in the spring of 2019. Assays were repeated at least three times independently.

Genome analysis of *P. orientalis* F9. The genome of *P. orientalis* F9 (CP018049.1) was analyzed for additional metabolites and factors with potential antagonistic activity using the Virulence Factors Database (VFDB; virulence factors of bacterial pathogens) and antiSMASH. In addition, blastn/tblastn (NCBI) comparison of the *P. orientalis* F9 genome and synthesis genes for additional secondary siderophores of pseudomonads was also performed using the sequences for enantio-pyochelin (47), pseudomonine (48), pyridine-2,6-bis(monothiocarboxylic acid) (PDTC) (49), and thioquinolobactin (50) synthesis genes.

SUPPLEMENTAL MATERIAL

Supplemental material is available online only.

SUPPLEMENTAL FILE 1, PDF file, 0.5 MB.

ACKNOWLEDGMENTS

We thank Elisabeth Eugster Meier and Barbara Guggenbühl for launching the Agroscope research program, Microbial Diversity (MikBioDiv), that made this work possible and Monika Maurhofer for providing *P. protegens* CHA0.

REFERENCES

1. Zengerer V, Schmid M, Bieri M, Müller DC, Remus-Emsermann MNP, Ahrens CH, Pelludat C. 2018. Pseudomonas orientalis F9: a potent antagonist against phytopathogens with phytotoxic effect in the apple flower. Front Microbiol 9:145. https://doi.org/10.3389/FMICB.2018.00145.
2. Vanneste JL (ed). 2000. Fire blight: the disease and its causative agent, *Erwinia amylovora*. CABI, Wallingford, United Kingdom.
3. McManus PS, Stockwell VO, Sundin GW, Jones AL. 2002. Antibiotic use in plant agriculture. Annu Rev Phytopathol 40:443–465. https://doi.org/10.1146/annurev.phyto.40.120301.093927.
4. Chiou CS, Jones AL. 1995. Expression and identification of the *strA-strB* gene pair from streptomycin-resistant *Erwinia amylovora*. Gene 152:47–51. https://doi.org/10.1016/0378-1119(94)00721-4.
5. Sundin GW, Werner NA, Yoder KS, Aldwinckle HS. 2009. Field evaluation of biological control of fire blight in the eastern United States. Plant Dis 93:386–394. https://doi.org/10.1094/PDIS-93-4-0386.
6. Mazzola M, Cook RJ, Thomashow LS, Weller DM, Pierson LS, III. 1992. Contribution of phenazine antibiotic biosynthesis to the ecological competence of fluorescent pseudomonads in soil habitats. Appl Environ Microbiol 58:2616–2624. https://doi.org/10.1128/AEM.58.8.2616-2624.1992.
7. Pierson LS, III, Thomashow LS. 1992. Cloning and heterologous expression of the phenazine biosynthetic locus from *Pseudomonas aureofaciens* 30-84. Mol Plant Microbe Interact 5:330–339. https://doi.org/10.1094/mpmi-5-330.
8. Parejko JA, Mavrodi DV, Mavrodi OV, Weller DM, Thomashow LS. 2012. Population structure and diversity of phenazine-1-carboxylic acid producing fluorescent *Pseudomonas* spp. from dryland cereal fields of central Washington State (USA). Microb Ecol 64:226–241. https://doi.org/10.1007/s00248-012-0015-0.
9. Velasco A, Acebo P, Gomez A, Schleissner C, Rodríguez P, Aparicio T, Conde S, Muñoz R, de la Calle F, Garcia JL, Sánchez-Puelles JM. 2005. Molecular characterization of the safracin biosynthetic pathway from *Pseudomonas fluorescens* A2-2: designing new cytotoxic compounds. Mol Microbiol 56:144–154. https://doi.org/10.1111/j.1365-2958.2004.04433.x.
10. Tang G-L, Tang M-C, Song L-Q, Zhang Y. 2016. Biosynthesis of tetrahydroisoquinoline antibiotics. Curr Top Med Chem 16:1717–1726. https://doi.org/10.2174/1568026616666151012112329.
11. Cornelis P, Matthijs S. 2002. Diversity of siderophore-mediated iron uptake systems in fluorescent pseudomonads: not only pyoverdines. Environ Microbiol 4:787–798. https://doi.org/10.1046/j.1462-2920.2002.00369.x.
12. Cornelis P. 2010. Iron uptake and metabolism in pseudomonads. Appl Microbiol Biotechnol 86:1637–1645. https://doi.org/10.1007/s00253-010-2550-2.
13. Haas D, Défago G. 2005. Biological control of soil-borne pathogens by fluorescent pseudomonads. Nat Rev Microbiol 3:307–319. https://doi.org/10.1038/nrmicro1129.
14. Pusey PL, Stockwell VO, Reardon CL, Smits THM, Duffy B. 2011. Antibiosis activity of *Pantoea agglomerans* biocontrol strain E325 against *Erwinia amylovora* on apple flower stigmas. Phytopathology 101:1234–1241. https://doi.org/10.1094/PHYTO-09-10-0253.
15. Takikawa Y, Serizawa S, Ichikawa T, Tsuyumu S, Goto M. 1989. *Pseudomonas syringae* pv. *actinidiae* pv. nov.: the causal bacterium of canker of kiwifruit in Japan. Jpn J Phytopathol 55:437–444. https://doi.org/10.3186/jjphytopath.55.437.
16. Ishimaru CA. 1988. Multiple antibiotic production by *Erwinia herbicola*. Phytopathology 78:746. https://doi.org/10.1094/Phyto-78-746.
17. Young JM. 1988. *Pseudomonas syringae* pv. *persicae* from nectarine,

peach, and Japanese plum in New Zealand. Bull OEPP 18:141–151. https://doi.org/10.1111/j.1365-2338.1988.tb00359.x.
18. Feistner GJ, Stahl DC, Gabrik AH. 1993. Proferrioxamine siderophores of *Erwinia amylovora*. A capillary liquid chromatographic/electrospray tandem mass spectrometric study. Org Mass Spectrom 28:163–175. https://doi.org/10.1002/oms.1210280307.
19. Kachadourian R, Dellagi A, Laurent J, Bricard L, Kunesch G, Expert D. 1996. Desferrioxamine-dependent iron transport in *Erwinia amylovora* CFBP1430: cloning of the gene encoding the ferrioxamine receptor FoxR. Biometals 9:143–150. https://doi.org/10.1007/bf00144619.
20. Smits THM, Duffy B. 2011. Genomics of iron acquisition in the plant pathogen *Erwinia amylovora*: insights in the biosynthetic pathway of the siderophore desferrioxamine E. Arch Microbiol 193:693–699. https://doi.org/10.1007/s00203-011-0739-0.
21. Dellagi A, Brisset MN, Paulin JP, Expert D. 1998. Dual role of desferrioxamine in *Erwinia amylovora* pathogenicity. Mol Plant Microbe Interact 11:734–742. https://doi.org/10.1094/MPMI.1998.11.8.734.
22. Guerinot ML, Meidl EJ, Plessner O. 1990. Citrate as a siderophore in *Bradyrhizobium japonicum*. J Bacteriol 172:3298–3303. https://doi.org/10.1128/jb.172.6.3298-3303.1990.
23. Balado M, Puentes B, Couceiro L, Fuentes-Monteverde JC, Rodríguez J, Osorio CR, Jiménez C, Lemos ML. 2017. Secreted citrate serves as iron carrier for the marine pathogen *Photobacterium damselae* subsp *damselae*. Front Cell Infect Microbiol 7:361. https://doi.org/10.3389/fcimb.2017.00361.
24. LeTourneau MK, Marshall MJ, Grant M, Freeze PM, Strawn DG, Lai B, Dohnalkova AC, Harsh JB, Weller DM, Thomashow LS. 2019. Phenazine-1-carboxylic acid-producing bacteria enhance the reactivity of iron minerals in dryland and irrigated wheat rhizospheres. Environ Sci Technol 53:14273–14284. https://doi.org/10.1021/acs.est.9b03962.
25. Miethke M, Marahiel MA. 2007. Siderophore-based iron acquisition and pathogen control. Microbiol Mol Biol Rev 71:413–451. https://doi.org/10.1128/MMBR.00012-07.
26. Neilands JB. 1995. Siderophores: structure and function of microbial iron transport compounds. J Biol Chem 270:26723–26726. https://doi.org/10.1074/jbc.270.45.26723.
27. Miller MB, Bassler BL. 2001. Quorum sensing in bacteria. Annu Rev Microbiol 55:165–199. https://doi.org/10.1146/annurev.micro.55.1.165.
28. Tyc O, van den Berg M, Gerards S, van Veen JA, Raaijmakers JM, de Boer W, Garbeva P. 2014. Impact of interspecific interactions on antimicrobial activity among soil bacteria. Front Microbiol 5:567. https://doi.org/10.3389/fmicb.2014.00567.
29. Venturi V. 2006. Regulation of quorum sensing in *Pseudomonas*. FEMS Microbiol Rev 30:274–291. https://doi.org/10.1111/j.1574-6976.2005.00012.x.
30. Meyers E, Cooper R, Trejo WH, Georgopapadakou N, Sykes RB. 1983. EM5519, a new broad-spectrum antibiotic produced by *Pseudomonas fluorescens*. J Antibiot (Tokyo) 36:190–193. https://doi.org/10.7164/antibiotics.36.190.
31. Zachow C, Jahanshah G, de Bruijn I, Song C, Ianni F, Pataj Z, Gerhardt H, Pianet I, Lämmerhofer M, Berg G, Gross H, Raaijmakers JM. 2015. The novel lipopeptide poaeamide of the endophyte *Pseudomonas poae* RE*1-1-14 is involved in pathogen suppression and root colonization. Mol Plant Microbe Interact 28:800–810. https://doi.org/10.1094/MPMI-12-14-0406-R.
32. Wells JS, Trejo WH, Principe PA, Sykes RB. 1984. Obafluorin, a novel beta-lactone produced by *Pseudomonas fluorescens*. Taxonomy, fermentation and biological properties. J Antibiot (Tokyo) 37:802–803. https://doi.org/10.7164/antibiotics.37.802.
33. Murdoch SL, Trunk K, English G, Fritsch MJ, Pourkarimi E, Coulthurst SJ. 2011. The opportunistic pathogen *Serratia marcescens* utilizes type VI secretion to target bacterial competitors. J Bacteriol 193:6057–6069. https://doi.org/10.1128/JB.05671-11.
34. Vogel C, Bodenhausen N, Gruissem W, Vorholt JA. 2016. The Arabidopsis leaf transcriptome reveals distinct but also overlapping responses to colonization by phyllosphere commensals and pathogen infection with impact on plant health. New Phytol 212:192–207. https://doi.org/10.1111/nph.14036.
35. Paternoster T, Défago G, Duffy B, Gessler C, Pertot I. 2010. Selection of a biocontrol agent based on a potential mechanism of action: degradation of nicotinic acid, a growth factor essential for *Erwinia amylovora*. Int Microbiol 13:195–206. https://doi.org/10.2436/20.1501.01.126.
36. King EO, Ward MK, Raney DE. 1954. Two simple media for the demonstration of pyocyanin and fluorescin. J Lab Clin Med 44:301–307.
37. Badarinarayana V, Estep PW, III, Shendure J, Edwards J, Tavazoie S, Lam F, Church GM. 2001. Selection analyses of insertional mutants using subgenic-resolution arrays. Nat Biotechnol 19:1060–1065. https://doi.org/10.1038/nbt1101-1060.
38. Holenstein G. 2009. A putative *Bradyrhizobium japonicum* metalloprotease: highly conserved, largely enigmatic. PhD dissertation. Eidgenössische Technische Hochschule, Zurich, Switzerland.
39. Born Y, Remus-Emsermann MNP, Bieri M, Kamber T, Piel J, Pelludat C. 2016. Fe^{2+} chelator proferrorosamine A: a gene cluster of *Erwinia rhapontici* P45 involved in its synthesis and its impact on growth of *Erwinia amylovora* CFBP1430. Microbiology 162:236–245. https://doi.org/10.1099/mic.0.000231.
40. Altschul SF, Gish W, Miller W, Myers EW, Lipman DJ. 1990. Basic local alignment search tool. J Mol Biol 215:403–410. https://doi.org/10.1016/S0022-2836(05)80360-2.
41. Skorupski K, Taylor RK. 1996. Positive selection vectors for allelic exchange. Gene 169:47–52. https://doi.org/10.1016/0378-1119(95)00793-8.
42. Galán JE, Ginocchio C, Costeas P. 1992. Molecular and functional characterization of the *Salmonella* invasion gene *invA*: homology of InvA to members of a new protein family. J Bacteriol 174:4338–4349. https://doi.org/10.1128/jb.174.13.4338-4349.1992.
43. Miller VL, Mekalanos JJ. 1988. A novel suicide vector and its use in construction of insertion mutations: osmoregulation of outer membrane proteins and virulence determinants in *Vibrio cholerae* requires *toxR*. J Bacteriol 170:2575–2583. https://doi.org/10.1128/jb.170.6.2575-2583.1988.
44. Schwyn B, Neilands JB. 1987. Universal chemical assay for the detection and determination of siderophores. Anal Biochem 160:47–56. https://doi.org/10.1016/0003-2697(87)90612-9.
45. Rosendahl CN, Olson LW. 1992. An *in vivo* screening method for antifungal activity against the plant pathogen *Pythium ultimum*. J Phytopathol 134:324–328. https://doi.org/10.1111/j.1439-0434.1992.tb01240.x.
46. Pusey PL. 1997. Crab apple blossoms as a model for research on biological control of fire blight. Phytopathology 87:1096–1102. https://doi.org/10.1094/PHYTO.1997.87.11.1096.
47. Youard ZA, Mislin GLA, Majcherczyk PA, Schalk IJ, Reimmann C. 2007. *Pseudomonas fluorescens* CHA0 produces enantio-pyochelin, the optical antipode of the *Pseudomonas aeruginosa* siderophore pyochelin. J Biol Chem 282:35546–35553. https://doi.org/10.1074/jbc.M707039200.
48. Mercado-Blanco J, van der Drift KM, Olsson PE, Thomas-Oates JE, van Loon LC, Bakker PA. 2001. Analysis of the *pmsCEAB* gene cluster involved in biosynthesis of salicylic acid and the siderophore pseudomonine in the biocontrol strain *Pseudomonas fluorescens* WCS374. J Bacteriol 183:1909–1920. https://doi.org/10.1128/JB.183.6.1909-1920.2001.
49. Lewis TA, Leach L, Morales S, Austin PR, Hartwell HJ, Kaplan B, Forker C, Meyer J-M. 2004. Physiological and molecular genetic evaluation of the dechlorination agent, pyridine-2,6-bis(monothiocarboxylic acid) (PDTC) as a secondary siderophore of *Pseudomonas*. Environ Microbiol 6:159–169. https://doi.org/10.1046/j.1462-2920.2003.00558.x.
50. Matthijs S, Baysse C, Koedam N, Tehrani KA, Verheyden L, Budzikiewicz H, Schäfer M, Hoorelbeke B, Meyer J-M, De Greve H, Cornelis P. 2004. The *Pseudomonas* siderophore quinolobactin is synthesized from xanthurenic acid, an intermediate of the kynurenine pathway. Mol Microbiol 52:371–384. https://doi.org/10.1111/j.1365-2958.2004.03999.x.
51. Imperiali N, Dennert F, Schneider J, Laessle T, Velatta C, Fesselet M, Wyler M, Mascher F, Mavrodi O, Mavrodi D, Maurhofer M, Keel C. 2017. Relationships between root pathogen resistance, abundance and expression of antimicrobial genes, and soil properties in representative Swiss agricultural soils. Front Plant Sci 8:427. https://doi.org/10.3389/fpls.2017.00427.
52. Simon R, Priefer U, Pühler A. 1983. A broad host range mobilization system for *in vivo* genetic engineering: transposon mutagenesis in gram negative bacteria. Nat Biotechnol 1:784–791. https://doi.org/10.1038/nbt1183-784.